Iranian Journal of Basic Medical Sciences
ijbms.mums.ac.ir

Modulation of autophagy and PI3K/Akt/mTOR pathway by naringin in sepsis-induced acute kidney injury

Ali Tugrul Akin [1, 2*], Zeynep Yilmaz [3], Emin Kaymak [4], Şaban Varinli [5], Esra Onal [6], Necla Deger [6], Meryem Sayan [6], Derya Karabulut [7], Zuleyha Doganyigit [4], Ayse Toluk [8]

[1] Istinye University, Faculty of Medicine, Department of Medical Biology, Istanbul, Turkey
[2] King's College London, Cancer and Pharmaceutical Sciences, The Rayne Institute, London, UK
[3] Erciyes University, Genome and Stem Cell Center, Kayseri, Turkey
[4] Yozgat Bozok University, Faculty of Medicine, Histology-Embryology Department, Yozgat, Turkey
[5] Yozgat Bozok University, Graduate School of Health Sciences, Histology-Embryology Department, Yozgat, Turkey
[6] Erciyes University, Graduate School of Health Sciences, Histology-Embryology Department, Kayseri, Turkey
[7] Erciyes University, Faculty of Medicine, Histology-Embryology Department, Kayseri, Turkey
[8] Erciyes University, Faculty of Science, Department of Biology, Kayseri, Turkey

ARTICLE INFO

Article type:
Original

Article history:
Received: Feb 13, 2026
Accepted: Jul 1, 2026

Keywords:
Acute kidney injury
Autophagy
Inflammation
Naringin
Sepsis

ABSTRACT

Objective(s): Sepsis-induced acute kidney injury (SI-AKI) is a life-threatening complication with limited treatment options, contributing to high morbidity and mortality worldwide. This study explores the renoprotective effects of naringin (NRG), a bioactive flavonoid, in a rat model of SI-AKI. It hypothesizes that NRG mitigates renal damage by enhancing autophagy and modulating the PI3K/Akt/mTOR pathway, thereby reducing oxidative stress, inflammation, and cellular injury.

Materials and Methods: Rats were divided into Control, NRG, LPS, LPS+NRG, and LPS+NRG+3-MA groups. NRG (100 mg/kg) was administered for 14 days, while LPS (10 mg/kg) induced sepsis. The LPS+NRG+3-MA group received 3-MA (30 mg/kg) to inhibit autophagy. Histopathological, immunohistochemical, gene expression, and biochemical analyses were performed. LPS-induced sepsis caused severe renal injury, including inflammation, tubular dilation, and oxidative stress (increased MDA, decreased catalase), alongside elevated TNF-α, NGAL, and KIM-1.

Results: NRG treatment significantly preserved renal structure, reduced oxidative stress, and lowered TNF-α, NGAL, and KIM-1 levels. Immunohistochemistry showed increased Beclin-1 and LC3 expression in the LPS+NRG group, suggesting enhanced autophagy. Gene expression analysis revealed activation of the PI3K/Akt/mTOR pathway in NRG-treated rats.

Conclusion: These findings indicate that NRG protects against SI-AKI by promoting autophagy and activating pro-survival pathways, offering a novel therapeutic strategy for sepsis management by regulating autophagy and modulating pathways.

▶ Please cite this article as:
Akin AT, Yilmaz Z, Kaymak E, Varinli Ş, Onal E, Deger N, Sayan M, Karabulut D, Doganyigit Z, Toluk A. Modulation of autophagy and PI3K/Akt/mTOR pathway by naringin in sepsis-induced acute kidney injury. Iran J Basic Med Sci 2026; 29:

Introduction

Sepsis-induced acute kidney injury (SI-AKI) is a critical condition marked by significant morbidity and mortality. Currently, no specific treatments exist for SI-AKI, and management is limited to supportive care (1). SI-AKI is a rapidly evolving disorder with a high prevalence and elevated mortality risk (2). It is estimated that approximately 19 million people worldwide experience sepsis annually, with nearly one-third developing AKI (3). Beyond its immediate life-threatening consequences, SI-AKI significantly increases the risk of progression to chronic kidney disease, imposing a long-term burden on patients and healthcare systems (4). When bacteria invade the body, the immune system can become overly reactive and lose balance, unleashing a surge of inflammatory signals. This excessive response activates both the complement system and key immune cells, setting the stage for SI-AKI (5). Research suggests that poor blood flow at the organ level is a major driver of SI-AKI. A severe drop in blood pressure, combined with reduced blood flow to the kidneys, can deprive kidney cells of oxygen and nutrients, ultimately leading to acute tubular damage and kidney dysfunction (6).

Autophagy is a key process by which cells maintain homeostasis by removing and reprocessing damaged organelles and other intracellular components, particularly under stress conditions such as nutrient deprivation (7), metabolic imbalance and apoptosis (8), and inflammation (9). This protective mechanism plays a crucial role in maintaining cell viability. Evidence from both clinical and preclinical studies indicates that sepsis triggers apoptosis across various organs, including the kidneys (10, 11). Moreover, growing evidence suggests that pharmacological

*Corresponding author: Ali Tugrul Akin. Istinye University, Faculty of Medicine, Department of Biology, Istanbul, Turkey, Cancer and Pharmaceutical Sciences, The Rayne Institute, King's College London, United Kingdom. Email: tugrul.akinn@gmail.com

stimulation of autophagy may serve as a protective strategy against SI-AKI (12). In the early stages of sepsis-related acute kidney injury (AKI), autophagosomes form and play a protective role by inhibiting various forms of programmed cell death. However, as the disease progresses and autophagic activity declines, programmed cell death pathways become activated, contributing to kidney injury and dysfunction. A study using a rat model of cecal ligation and puncture-induced sepsis revealed that autophagy was initially up-regulated, peaking at 4 hr, then declined after 9 hr. This decrease in autophagic activity correlated with increased apoptosis in proximal renal tubular cells, suggesting that sustained autophagy may help protect kidney function during sepsis (13).

The PI3K/Akt/mTOR signaling pathway plays a pivotal role in regulating essential cellular processes, including metabolism, proliferation, apoptosis, survival, and protein synthesis. Growing evidence suggests that activation of this pathway may confer renal protection against ischemia-reperfusion injury (14). PIK3CA is responsible for encoding the p110α catalytic subunit of PI3K, a pivotal enzyme that participates in signaling cascades influencing cell proliferation, growth, survival, and metabolic activity. Akt is a key regulator of the interplay between autophagy and apoptosis, processes that contribute to the progression of both systemic and localized inflammation (15). mTOR serves as a key regulator of cellular growth and metabolism, coordinating signals from nutrients, growth factors, and energy availability to modulate anabolic processes, including protein synthesis and lipid metabolism, particularly under nutrient-rich conditions (16). Conversely, under conditions of nutrient deprivation or cellular stress, mTOR is inhibited, thereby activating autophagy as a survival mechanism (17).

The complex formed by lipopolysaccharide (LPS) and its binding protein activates membrane CD14 and toll-like receptors (TLRs) such as TLR4 on immune cells, triggering a signaling cascade that enhances nuclear factor-κB (NF-κB) activity (18). NF-κB is an important transcription factor driving the expression of numerous proinflammatory cytokines, chemokines, and adhesion molecules (19). Activation of TLR4 by LPS results in NF-κB entering the nucleus, where it promotes increased expression of key pro-inflammatory cytokines—IL-6 and TNF-α—that drive the inflammatory response associated with LPS-induced sepsis (20). This activation plays a pivotal role in sepsis-induced inflammation, causing a widespread surge of immune mediators—often referred to as a "cytokine storm"—that contributes to AKI and increases the mortality risk.

A wide range of biomarkers has been identified to support early detection and risk stratification in acute kidney injury (AKI). Key markers reflecting tubular damage include NGAL, KIM-1, and liver-type fatty acid-binding protein (L-FABP)(21, 22). These biomarkers play a crucial role in assessing kidney function, predicting injury severity, and guiding therapeutic interventions (23). Besides NGAL and KIM-1, numerous studies have shown that SI-AKI causes notable changes in kidney function markers—including blood urea nitrogen (BUN), creatinine, and uric acid—which rise in the serum due to reduced renal filtration (24). These biomarkers serve as critical indicators for evaluating kidney dysfunction and the extent of renal damage.

Naringin (NRG) is a flavanone glycoside consisting of the flavanone naringenin linked to the disaccharide neohesperidose. It is a biologically active compound predominantly found in traditional Chinese medicinal plants, including *Drynaria fortunei* (Kunze) J. Sm. (DF), *Citrus aurantium* L. (CA) and *Citrus medica* L. (CM). Additionally, NRG is abundant in citrus fruits, where it contributes to their distinctive bitter flavor (25). A variety of pharmacological effects have been attributed to NRG, among them antioxidant, antimicrobial, anticancer, anti-inflammatory, antiulcer, antiapoptotic, hepatoprotective, antidiabetic, and lipid-modulating functions (26). Beyond its sensory properties, NRG is considered an important dietary flavonoid, as citrus fruits are widely consumed worldwide and represent a major source of natural antioxidants in the human diet. Regular intake of NRG through fruit consumption has been associated with potential health benefits, including anti-inflammatory and renoprotective effects, highlighting its relevance as a functional food component in human nutrition (27).

Given the critical role of autophagy in cellular homeostasis and its emerging significance in protecting against sepsis-induced organ damage, we hypothesized that NRG, a bioactive flavonoid with known antioxidant and anti-inflammatory properties, could mitigate SI-AKI by shifting the balance from apoptosis to autophagy in the early stages of sepsis. This study aims to investigate the renoprotective effects of NRG in a rat model of SI-AKI, focusing on its ability to modulate key cellular survival pathways, including the PI3K/Akt/mTOR signaling pathway. To test our hypothesis, we employed a comprehensive approach that integrated histopathological, immunohistochemical, gene expression, and biochemical analyses. Histological and immunohistochemical staining were performed to assess tissue integrity and expression of autophagy and apoptosis markers. Quantitative PCR was used to assess the transcriptional regulation of key signaling molecules, while ELISA was used to measure oxidative stress and inflammatory mediators. Our findings provide insights into the potential therapeutic application of NRG in SI-AKI, offering a novel strategy to mitigate acute kidney injury by regulating autophagy.

Materials and Methods

Chemicals

Lipopolysaccharide (LPS) from Escherichia coli (Sigma-Aldrich, Catalog No: L2630, Merck, Darmstadt, Germany) was reconstituted in distilled water to prepare a stock solution. NRG, with a purity greater than 98%, was obtained as a powder from Sigma-Aldrich (Catalog No: 71162-100G, Merck, Darmstadt, Germany). To ensure stability and solubility, it was first dissolved in ethanol at a safe concentration (<1 g/ml), as reported by Rivier (1993), and then diluted in physiological serum. 3-Methyladenine (3-MA)(Sigma-Aldrich, Catalog No: M9281-100MG, Merck, Darmstadt, Germany) was solubilized in distilled water before use. All stock solutions were freshly prepared or stored under appropriate conditions to maintain stability and experimental consistency.

Experimental design

The research protocol received approval from the Erciyes University Experimental Animal and Local Ethics Committee (Ref: 21/102/2021). All procedures involving animals adhered to ethical guidelines ensuring humane

treatment. In this experimental study, forty male Wistar Albino rats, each approximately nine weeks old and weighing between 200 and 250 grams, sourced from the Hakan Cetinsaya Experimental and Clinical Research Center at Erciyes University, Kayseri, Turkey, were used. The rats were maintained under standard laboratory conditions, including a controlled 12-hour light/dark cycle, ambient temperatures of 20-24 ˚C, and appropriate humidity levels. They had unrestricted access to drinking water and a nutritionally balanced laboratory diet. The animals were randomly distributed into four experimental groups (n=10 per group). The Control group consisted of untreated rats, while the NRG group received 100 mg/kg of NRG intraperitoneally (IP) for 14 days (28). The LPS group was administered 10 mg/kg IP lipopolysaccharide (LPS) on day 14 after the final dose of NRG (29). The LPS+NRG group received 10 mg/kg IP LPS on day 14, followed by a 14-day NRG regimen. Additionally, the LPS+NRG+3-MA group was administered the previously specified doses of LPS and NRG, along with 30 mg/kg of 3-methyladenine (3-MA). To evaluate the autophagy-inducing effects of NRG, the autophagy inhibitor 3-MA was administered 30 min before LPS injection as part of the experimental protocol (30). After the administrations, the rats were monitored for 6 hr to observe signs of sepsis, including reduced activity, muscle weakness, lethargy, and other abnormal behaviors. Body temperatures of the LPS-treated rats were also recorded. Upon confirmation of sepsis symptoms, anesthesia was performed by intraperitoneal administration of ketamine (30 mg/kg) and xylazine (4 mg/kg), and kidney tissues and blood samples were collected for further analysis. The experimental design is shown in Figure 1.

Histopathological evaluation

Kidney samples collected from the animals were preserved in a 4% formaldehyde solution for histological evaluation. The fixed tissues then underwent a series of processing steps, including dehydration, clearing, and paraffin embedding. Thin sections, 5 µm thick, were cut from the paraffin-embedded blocks. These sections were subsequently stained and analyzed under a light microscope (Olympus BX51, Center Valley, PA) to assess histopathological alterations, and photomicrographs were captured for documentation (31).

Hematoxylin and eosin staining (H&E)

Tissue sections were deparaffinized by incubating them at 58 ˚C for two hours. Following deparaffinization, the sections were rehydrated through a graded alcohol series and subsequently rinsed with tap water. Hematoxylin and eosin (H&E) staining was performed at room temperature. After completing the dehydration, clearing, and coverslipping steps, all sections were examined under a light microscope to evaluate histological alterations in kidney tissues across the experimental groups (32).

Kidney injury score

For the histopathological assessment of kidney sections, the following criteria were employed: mononuclear cell infiltration, hemorrhage, proximal tubule dilatation, and glomerular degeneration. Scoring was performed using the following scale: 0=absent; 1=0-25%; 2=26-45%; 3=46-75%; and 4=76-100% involvement (33). The quantitative data from scoring all sections for the experimental groups were examined and statistically compared across groups.

Immunohistochemical staining

Immunohistochemistry was conducted to evaluate the expression levels of Beclin-1, LC3, and Caspase-3 in kidney tissue. Tissue sections were initially deparaffinized by incubating them in an oven at 60 ˚C for at least two hours. Further deparaffinization and rehydration were performed using xylene and a graded alcohol series, respectively. Antigen retrieval was performed by immersing the sections in 0.01 M citrate buffer and heating them in a microwave oven at 350 W. The sections were then rinsed three times with phosphate-buffered saline (PBS) for five minutes each. To block endogenous peroxidase activity, the samples were incubated in a 3% (w/v) hydrogen peroxide (H_2O_2) solution for 10 min, followed by three additional PBS washes. A blocking solution was applied for 10 min before incubating the sections overnight at 4 ˚C with primary antibodies targeting Beclin-1 (Cat. No: BS-1353R, Bioss, USA), LC3 (Cat. No: BS-8878R, Bioss, USA), and Caspase-3 (Cat. No: E-AB-66940, Elapscience, USA). The following morning, the sections were washed three times with PBS before being incubated with a secondary antibody (TA-125-HDX, Thermo Fisher Scientific, Waltham, MA, USA)

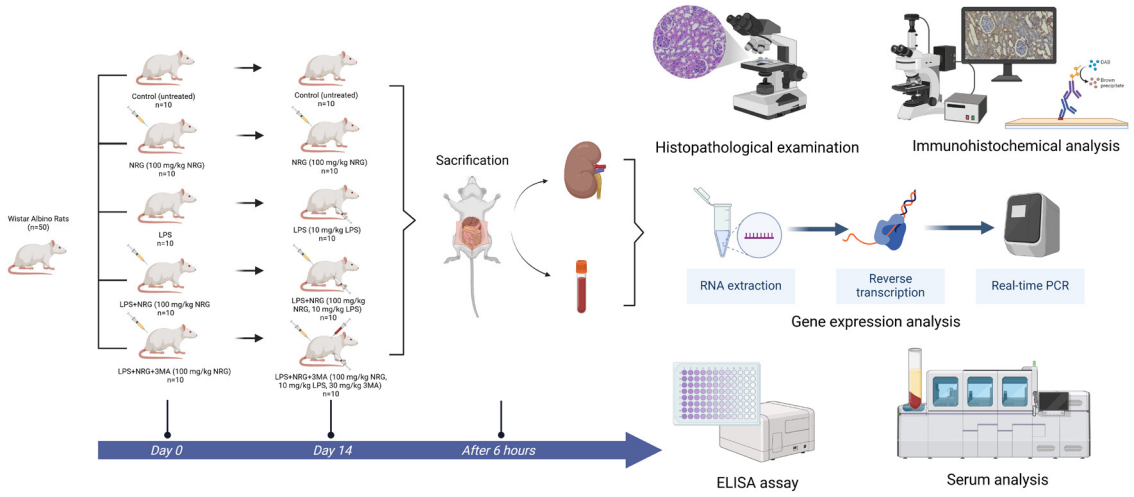

Figure 1. Schematic representation of the experimental design

for one hour at room temperature. Signal amplification was achieved using the streptavidin–avidin–peroxidase complex, and immunoreactivity was visualized with 3,3′-diaminobenzidine tetrahydrochloride (TA-060-HDX, Thermo Fisher Scientific, Waltham, MA, USA). The sections were counterstained with Gill hematoxylin, dehydrated through an increasing alcohol series, cleared in xylene, and mounted in Entellan for final analysis.

Semi-quantitative immunohistochemistry

All tissue sections from the experimental groups were analyzed for Beclin-1, LC3, and Caspase-3 immunoreactivity. For each group, images were captured from 100 microscopic fields. Immunoreactivity intensity was quantified using ImageJ software (version 1.45s, National Institute of Health, USA; RRID: SCR_003070). A total of 100 measurements of immunoreactivity density were recorded per marker in each group and subsequently evaluated. To facilitate comparisons between experimental groups, statistical analysis was performed on the collected quantitative data (34).

Gene expression analysis via quantitative PCR

Total RNA extraction from kidney tissue and cDNA synthesis

Total RNA extraction from the kidney was done using Qiazol™ Lysis Buffer (Qiagen, Germantown, MD, USA) according to the manufacturer's instructions. Briefly, kidney tissue samples were placed in 2 ml Eppendorf tubes and homogenized using 1 ml of Qiazol lysis buffer per 100 mg of tissue to ensure complete cell lysis and efficient RNA release. The homogenized samples underwent phase separation, followed by RNA precipitation and purification steps to obtain high-quality RNA. The concentration and purity of the extracted RNA were assessed using a NanoDrop 2000 spectrophotometer (Thermo Fisher Scientific, Waltham, MA, USA) by measuring the A260/A280 and A260/A230 absorbance ratios to confirm RNA integrity. The isolated RNA samples were stored at -80 ˚C until further use to prevent degradation. cDNA synthesis was performed using the EvoScript Universal cDNA Master Kit (Roche, Basel, Switzerland) following the manufacturer's protocol. In brief, the reaction mixture consisted of 4 µl of 5×-diluted reaction buffer, 11 µl of nuclease-free water, and 3 µl of RNA sample, with the final volume adjusted to 20 µL using 10×-diluted reaction buffer. Reverse transcription was conducted in a SensoQuest Thermal Cycler (SensoQuest, Göttingen, Germany) under the following conditions: 42 ˚C for 15 min, 85 ˚C for 5 min, and 65 ˚C for 15 min. After incubation, cDNA samples were diluted 1:5 in 80 µl of nuclease-free water and stored at -20 ˚C for subsequent gene expression analysis.

Quantification of gene expression via SYBR Green-based real-time PCR

Quantitative real-time PCR (qRT-PCR) was performed using the SYBR Green I Master Kit (Roche, Basel, Switzerland) according to the manufacturer's guidelines. The following gene-specific primers were employed: PIK3CA, encoding the p110α catalytic subunit of phosphatidylinositol 3-kinase (PI3K); Akt; and mTOR, with β-actin (ACTB) as the housekeeping gene for normalization. The reaction mixture (total volume: 18 µl) was prepared as follows: 10 µl SYBR Green Master Mix, 0.5 µl primer mix, and 7.5 µl RNase-free water. Subsequently, 2 µl of cDNA was added to the prepared reaction mixture, and amplification was performed using the LightCycler 480 II Real-Time PCR System (Roche, Basel, Switzerland). The obtained Ct (cycle threshold) values were normalized against β-actin (ACTB) to ensure consistency across samples. Relative gene expression was determined using the 2ΔΔCt method to compare gene expression among experimental groups (35).

Enzyme-linked immunosorbent assay (ELISA)

To assess oxidative stress and inflammatory markers, including malondialdehyde (MDA), catalase (CAT), tumor necrosis factor-alpha (TNF-α), neutrophil gelatinase-associated lipocalin (NGAL), and kidney injury molecule-1 (KIM-1), an ELISA assay was performed on kidney tissue samples. Rat-specific ELISA kits (MDA, Cat. No: ELK86132, ELK Biotechnology, Denver, CO, USA; CAT, Cat. No: ELK5986, ELK Biotechnology, Denver, CO, USA: TNF-α, Cat. No: E0764Ra, Bioassay Technology Laboratory, Shanghai, China: NGAL, Cat. No: E0762Ra, Bioassay Technology Laboratory, Shanghai, China: KIM-1, Cat. No: ELK2288 (ELK Biotechnology, Denver, CO, USA) was used for marker quantification. Quality control measures included internal and external controls provided in the kits, with negative and positive controls incorporated into each assay. Batch effects were minimized by processing all samples for each marker in a single run. Kidney tissue homogenates were centrifuged at 10,000 rpm for 15 min at 4 ˚C. Subsequently, 150 µl of the resulting supernatant was aliquoted into Eppendorf tubes. For standard preparation, five tubes were filled with standard diluent. A 120 µl volume of the standard solution was added to the first tube and mixed, after which 120 µl was sequentially transferred to the next four tubes. To prepare the sample, 40 µL of supernatant was added to the designated sample section, followed by 10 µL of antibody. The mixture was incubated at 37 ˚C for 60 min. Next, 50 µl of streptavidin-HRP was added to both the standard and sample sections, followed by a 10-minute incubation at 37 ˚C. Finally, solutions A and B, along with the stop solution, were sequentially added, and absorbance was measured using an ELISA reader (36).

Kidney function markers

Blood samples were centrifuged to isolate serum for further biochemical analysis. Isolated serum samples were stored at -80 ˚C until further examination. Kidney function markers, blood urea nitrogen (BUN), creatinine, and uric acid levels, were assessed by using the Roche™ Cobas 8000 Modular Analyzer system at the Erciyes University Central Biochemistry Laboratory. Statistical analysis was conducted on the obtained measurements to facilitate comparisons among groups.

Statistical analysis

All statistical analyses were performed using GraphPad Prism version 9.00 for Mac (GraphPad Software, La Jolla, CA, USA). The normality of data distribution was evaluated using the D'Agostino-Pearson omnibus test and the Shapiro-Wilk test. For datasets following a normal distribution, one-way analysis of variance (ANOVA) was conducted, whereas the Kruskal-Wallis test was employed for non-normally distributed data. Multiple comparisons were assessed using Tukey's *post hoc* test. Statistical significance was defined as a P-value<0.05.

Results

Naringin protects the kidneys against septic acute kidney injury

To assess the effects of NRG treatment on LPS-induced acute kidney injury, H&E-stained kidney tissues were examined for histopathological changes. The Control and NRG groups showed normal kidney tissue histology. In contrast, the LPS group exhibited significant histopathological alterations, including mononuclear cell infiltration, hemorrhage, proximal tubule dilation, and glomerular degeneration, resulting in a significant increase in kidney injury scores compared to the Control and NRG groups (P<0.0001)(Figure 2A, B). However, the kidney tissue morphology in the LPS+NRG and LPS+NRG+3-MA groups resembled that of the Control and NRG groups, with most histological changes observed in the LPS group being absent. Only minimal hemorrhage was detected in some areas of the LPS+NRG group (Figure 2A). Consequently, kidney injury in the LPS+NRG and LPS+NRG+3-MA groups was significantly lower compared to the LPS group (P<0.0001)(Figure 2B).

Increase in autophagy-related markers in kidney tissue by NRG pre-treatment

Immunohistochemical staining using the avidin-biotin technique was employed to examine changes in the expression of Beclin-1, LC3, and Caspase-3 in kidney tissue. All experimental groups showed detectable levels of Beclin-1, LC3, and Caspase-3, as confirmed by immunohistochemical staining and statistical analysis of the quantitative data obtained by the measurements of immunoreactivity intensity of these markers. In the NRG group, the expression levels of Beclin-1, LC3, and Caspase-3 were similar to those in the Control group. In contrast, the LPS group showed a slight increase in Caspase-3 immunoreactivity in their kidney tissue. However, this increase was not statistically significant. However, the LPS+NRG group had noticeably lower Caspase-3 levels compared to the LPS group. Moreover, the LPS+NRG+3-MA group showed relatively increased Caspase-3 immunoreactivity. Furthermore, Beclin-1 and LC3 expression levels were significantly higher in the LPS+NRG and LPS+NRG+3-MA groups, suggesting that NRG stimulates autophagy in the kidney. Figure 3A shows immunohistochemical staining for these markers, and Figure 3B presents the statistical analysis of immunoreactivity measurements across the experimental groups.

Naringin pre-treatment activates the P13K/Akt/mTOR pathway during septic acute kidney injury

Quantitative PCR was used to determine the expression levels of P13K, Akt, and mTOR in the kidney tissue. The results indicate no significant differences in the expression levels of PI3K, Akt, and mTOR between the Control and NRG groups. In contrast, the LPS group showed relatively lower expression of PI3K, Akt, and mTOR compared with both the Control and NRG groups. However, in the LPS+NRG and LPS+NRG+3-MA groups, significant increases in the expression of PI3K, Akt, and mTOR were observed compared with the LPS group. This suggests that the combination of LPS and NRG led to a marked activation of the PI3K/Akt/mTOR signaling pathway. Moreover, the LPS+NRG+3-MA group also showed high expression levels of PI3K, Akt, and mTOR. However, this increase was not significant when compared to that in the LPS+NRG group. The increase in these mRNA expression levels in the LPS+NRG and LPS+NRG+3-MA groups supports the hypothesis that NRG may exert its protective

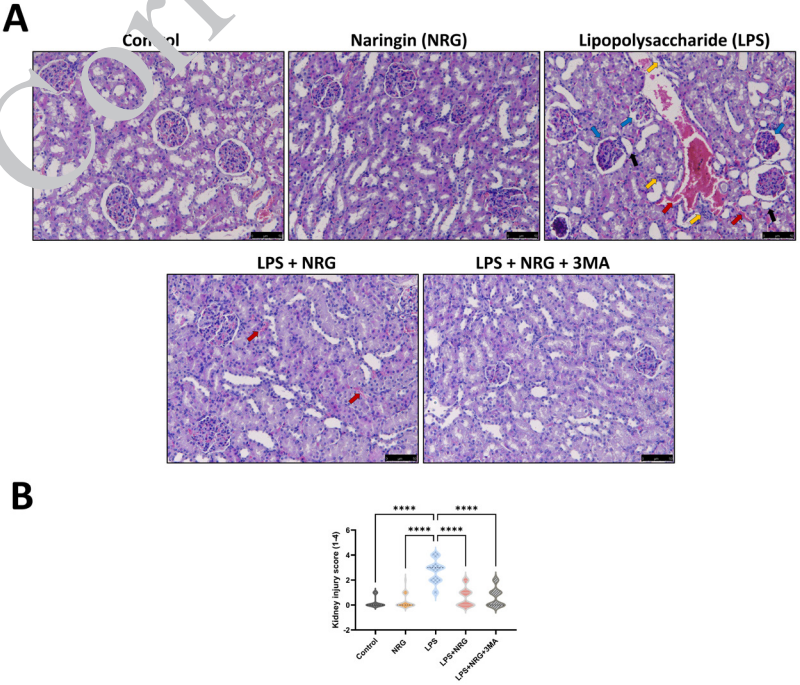

Figure 2. Light microscopy of H&E-stained kidney tissues and quantitative analysis of rat kidney injury scores
A. H&E staining of kidney tissues. Control (untreated rats) and NRG (100 mg/kg NRG) groups exhibited normal histological architecture. The LPS group (10 mg/kg lipopolysaccharide) displayed mononuclear cell infiltration (blue arrows), hemorrhage (red arrows), proximal tubule dilatation (green arrows), and glomerular degeneration (yellow arrows). The LPS+NRG and LPS+NRG+3-MA groups showed relatively healthy histological structures. B. Statistical analysis of kidney injury scores across experimental groups. Scale bar=50 µm. $^{*}P$<0.05, $^{**}P$<0.01, $^{***}P$<0.001, $^{****}P$<0.0001
NRG: naringin, LPS: lipopolysaccharide, 3MA: 3-metyladenine

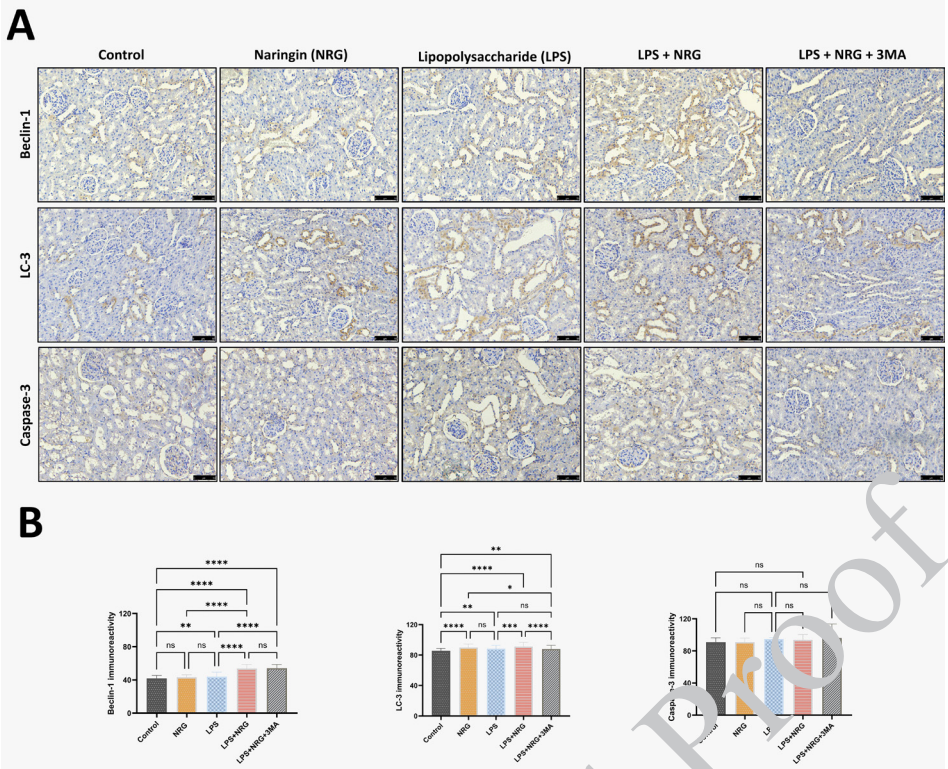

Figure 3. Immunohistochemical staining of Beclin-1, LC3, and Caspase-3 in kidney tissues (A) and the statistical analysis of the immunoreactivity measurements across the experimental groups (B)
Control and NRG groups showed weak staining for Beclin-1, LC3, and Caspase-3, whereas the LPS group showed increased expression of these markers. The LPS+NRG group exhibited higher expression levels comparable to those of the Control, NRG, and LPS groups. Scale bar: 50 µm. Significant differences were considered at $P<0.05$. $^{*}=P<0.05$, $^{**}=P<0.01$, $^{***}=P<0.001$, $^{****}=P<0.0001$
NRG: naringin, LPS: lipopolysaccharide, 3MA: 3-metyladenine

effects by modulating the PI3K/Akt/mTOR pathway. Figure 4 shows the expression levels of these markers among the experimental groups.

Attenuation of oxidative stress and inflammatory responses by NRG

To further elucidate the protective mechanisms of NRG in septic acute kidney injury, oxidative stress and inflammatory markers, including MDA, catalase, and TNF-α, were analyzed. MDA, a product of lipid peroxidation and a widely recognized marker of oxidative stress, was significantly elevated in the LPS group, indicating triggered oxidative damage in renal tissue. Furthermore, catalase, a critical antioxidant enzyme that neutralizes reactive oxygen species (ROS), showed a marked decrease in the LPS group, suggesting an imbalance between oxidative stress and the kidney's antioxidant defense mechanisms. Inflammatory responses were also assessed by measuring TNF-α, a pro-inflammatory cytokine. TNF-α levels were significantly elevated in the LPS group, reflecting an intense inflammatory response and cytokine overproduction. However, pre-treatment with NRG effectively mitigated these adverse effects. The LPS+NRG and LPS+NRG+3-MA groups exhibited significantly lower levels of MDA and TNF-α, with preserved catalase activity (Figure 5).

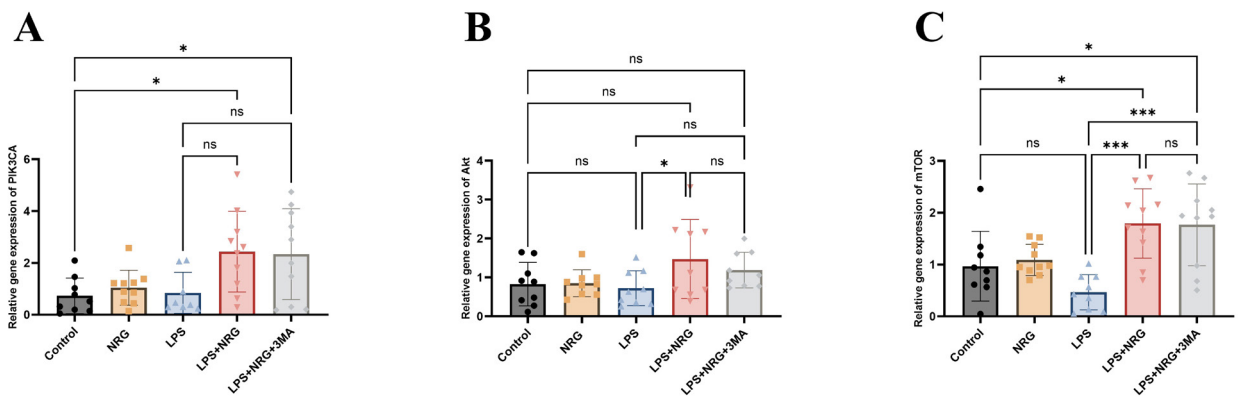

Figure 4. Relative gene expression analysis for PI3K, Akt, and mTOR in rat kidney tissue
The LPS group showed lower expression levels of these markers compared to the Control and NRG groups ($P<0.05$). The up-regulation of these markers was seen in the LPS+NRG and LPS+NRG+3-MA groups compared to the LPS group ($P<0.05$). Significant differences were considered at $P<0.05$. $^{*}=P<0.05$, $^{**}=P<0.01$, $^{***}=P<0.001$, $^{****}=P<0.0001$
PI3K: phosphoinositide 3-kinases, mTOR: mechanistic target of rapamycin, NRG: naringin, LPS: lipopolysaccharide, 3MA: 3-metyladenine

Naringin mediates the preservation of kidney function

Kidney function was evaluated by measuring changes in the serum levels of NGAL, KIM-1, BUN, creatinine, and uric acid, which are key indicators of renal health and filtration capacity. NGAL and KIM-1, biomarkers of acute kidney injury (AKI) and tubular damage, were elevated in the LPS group compared to the Control and NRG groups, indicating severe renal impairment. In particular, the increase in NGAL levels in the LPS group was statistically significant. Similarly, BUN and creatinine levels were markedly increased in the LPS group (P<0.05), suggesting a decline in glomerular filtration rate and reduced overall renal clearance capacity. However, uric acid levels exhibited an inverse pattern, showing a significant decrease in the LPS group. However, pre-treatment with NRG appeared to counteract these detrimental effects, as the LPS+NRG and LPS+NRG+3-MA groups demonstrated NGAL, KIM-1, BUN, creatinine, and uric acid levels comparable to those of the Control and NRG groups (Figures 5 and 6).

Discussion

SI-AKI fuels a dangerous cycle, each amplifying vulnerability to the other. While sepsis is the top trigger for AKI, developing AKI—no matter the cause—dramatically raises a patient's risk of life-threatening infections, including sepsis (37). Research has demonstrated that mitigating kidney damage and restoring kidney function can significantly reduce mortality among patients with sepsis (38). An increasing amount of research has demonstrated in recent years how crucial the inflammatory response is to the pathophysiology of sepsis. In particular, the release of inflammatory mediators, triggered by bacterial constituents

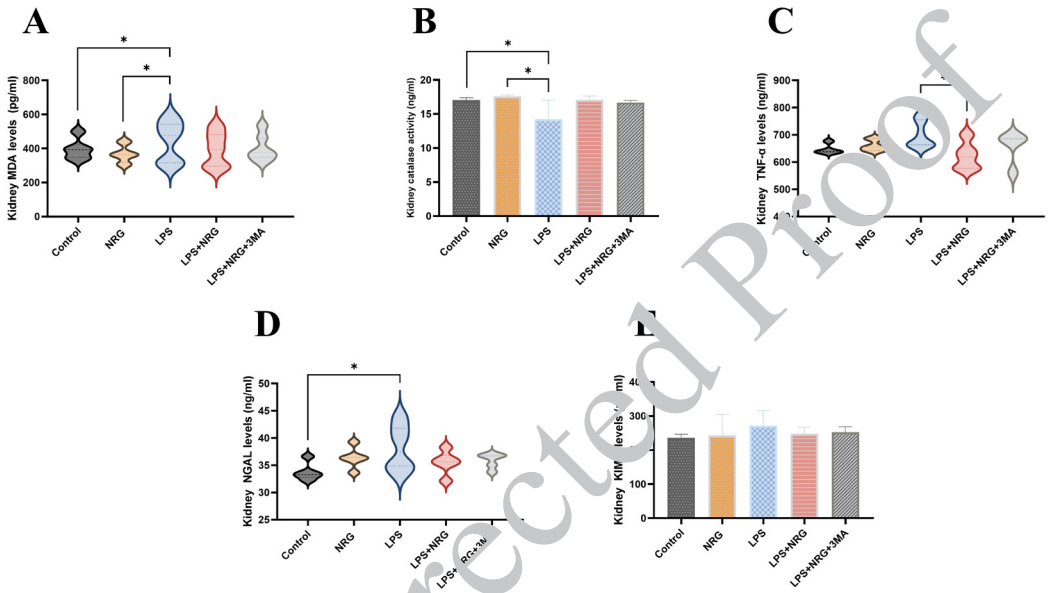

Figure 5. Statistical analysis of tissue levels of MDA, CAT, TNF-α, NGAL, and KIM-1 determined by ELISA across rat experimental groups
The LPS exhibited increased tissue MDA, TNF-α, NGAL, and KIM-1 levels, alongside decreased CAT levels, compared to the Control and NRG groups. The LPS+NRG and LPS+NRG+3-MA groups showed similar levels of these markers, comparable to those of the Control and NRG groups. Significant differences were considered at P<0.05. *=P<0.05 MDA: malondialdehyde, CAT: catalase, TNF-a: tumor necrosis factor alpha, NGAL: neutrophil galatinase-associated lipocalin, KIM-1: kidye injury molecule-1, NRG: naringin, LPS: lipopolysaccharide, 3MA: 3-metyladenine, ELISA: enzyme linked immunosorbent assay

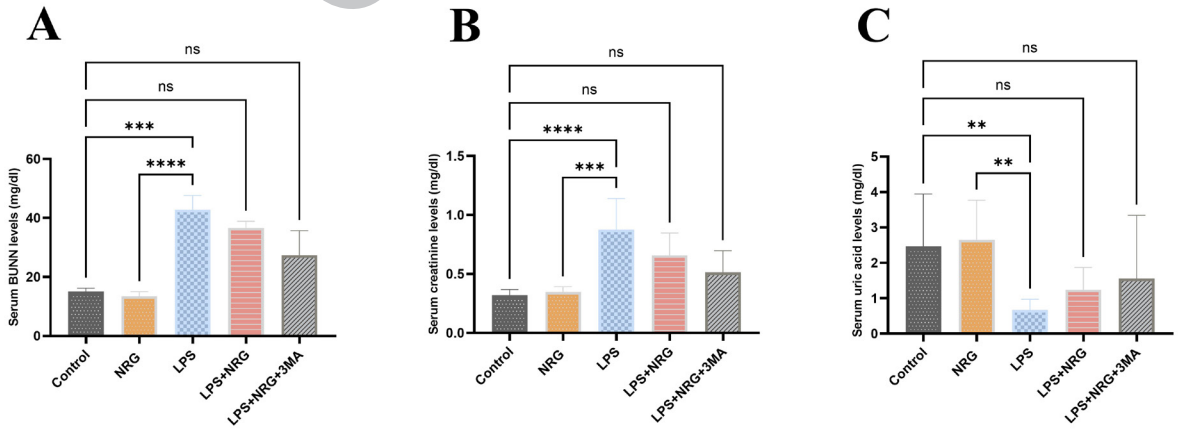

Figure 6. Measurements of serum BUN, creatinine, and uric acid levels obtained via biochemical assays, with statistical analysis across rat experimental groups
The LPS group showed increased serum BUN and creatinine levels and decreased uric acid levels compared to the Control and NRG groups. However, the levels of these markers in the LPS+NRG group were similar to those in the Control and NRG groups. Significant differences were considered at P<0.05. *=P<0.05, **=P<0.01, ***=P<0.001, ****=P<0.0001 NRG: naringin, LPS: lipopolysaccharide, 3MA: 3-metyladenine, BUN: blood urea nitrogen

such as LPS, drives this reaction (39). The cascade of events initiated by these mediators contributes to the systemic inflammation observed in sepsis, further complicating its clinical management. Moreover, sepsis-induced kidney dysfunction exacerbates the systemic inflammatory response, creating a vicious cycle that complicates patient outcomes. The kidney, a key organ for filtration and waste excretion, when impaired, leads to the accumulation of toxic metabolites and electrolyte imbalances. This, in turn, exacerbates the inflammatory response, contributing to the deterioration of other organ systems and increasing the likelihood of multiple organ failure. (40). In this study, we investigated NRG's renoprotective mechanisms, focusing on its ability to modulate autophagy—a cellular survival pathway—and its interaction with the PI3K/Akt/mTOR signaling axis. Our findings reveal that NRG not only attenuates oxidative stress and inflammation but also rebalances cellular homeostasis by enhancing autophagy in the early stages of the disease while paradoxically activating pro-survival mTOR signaling. This dual regulatory effect challenges conventional pathways, suggesting a unique therapeutic strategy to preserve renal function in sepsis.

Several studies showed that LPS-induced sepsis triggers profound renal structural damage, characterized by histopathological hallmarks such as mononuclear cell infiltration, glomerular degeneration, proximal tubule dilatation, and hemorrhage. These changes reflect the kidney's maladaptive response to systemic inflammation and LPS-driven oxidative stress in the first hours of the septic response (41). We hypothesized that NRG exerts renoprotective effects in SI-AKI by dampening oxidative stress and inflammatory responses via its antioxidant (42) and anti-inflammatory (43) properties. Our histopathological analysis supports the protective role of NRG in SI-AKI. LPS administration resulted in severe kidney damage, characterized by mononuclear cell infiltration, hemorrhage, proximal tubule dilation, and glomerular degeneration, as reflected by the significantly elevated kidney injury score. In contrast, NRG treatment markedly preserved renal architecture, reducing mononuclear cell infiltration, hemorrhage, proximal tubule dilation, and glomerular degeneration, suggesting its ability to mitigate LPS-induced damage. Interestingly, the addition of 3-MA, an autophagy inhibitor, partially diminished NRG's protective effect, suggesting that autophagy may be a crucial mechanism underlying NRG's renoprotective properties against renal tissue damage. These findings highlight the potential of NRG at the dose of 100 mg/kg as a therapeutic candidate for SI-AKI.

In the early stages of sepsis-related AKI, autophagosomes form and play a protective role by inhibiting various forms of programmed cell death. However, as the disease progresses and autophagic activity declines, programmed cell death pathways become activated, contributing to kidney injury and dysfunction (13). Our immunohistochemical findings indicate that autophagy-related markers are overexpressed in SI-AKI, as evidenced by increased Beclin-1 and LC3 expression in the LPS group compared with the Control group. This suggests that autophagy may be an adaptive response to LPS-induced cellular stress, potentially serving as a protective mechanism in kidney tissue to clear damaged organelles, consistent with previous studies (44). Interestingly, NRG further increases the expression levels of autophagy-related markers, as evidenced by significant up-regulation of Beclin-1 and LC3 in the LPS+NRG group during the early stages of sepsis. This implies that NRG may reinforce autophagic activity to promote cellular homeostasis and protect the kidney. However, when we inhibited autophagy by using 3-MA, Beclin-1 and LC3 expression levels were significantly reduced, confirming that NRG's potential effects on autophagy are specific and not secondary to other cellular processes. Notably, Caspase-3 expression remained unchanged across all groups, indicating that apoptosis is not the primary mechanism driving kidney injury in this model. Another limitation of the present study is that autophagy was evaluated by assessing the expression of autophagy-associated markers rather than by direct assessment of autophagic flux. Although NRG treatment increased Beclin-1 and LC3 expression, these findings alone are insufficient to conclusively demonstrate enhanced autophagic activity. Key parameters commonly used to verify autophagic flux, including the LC3-II/LC3-I ratio, p62/SQSTM1 degradation, and flux assays employing lysosomal inhibitors, were not assessed in the current study. Our results suggest that NRG's renoprotective effects at a dose of 100 mg/kg in SI-AKI are largely mediated by regulation of autophagy-related markers rather than by direct inhibition of apoptosis.

In the classical paradigm, the PI3K/Akt/mTOR pathway plays a central regulatory role in cell growth, metabolism, and survival, while autophagy is typically suppressed by mTOR activation (45). Under normal conditions, PI3K activates Akt, which in turn stimulates mTOR, leading to enhanced protein synthesis and inhibition of autophagy. Conversely, under conditions of nutrient deprivation or cellular stress, mTOR is inhibited, thereby activating autophagy as a survival mechanism (46). Our gene expression analyses showed that LPS-induced inflammation did not activate the PI3K/Akt/mTOR cascade in the kidney; however, treatment with 100 mg/kg NRG activated this pathway in the LPS+NRG group. This dual action of NRG suggests that stimulation of the PI3K/Akt/mTOR pathway may enhance cellular metabolism and survival while helping to prevent excessive autophagic degradation. Both mechanisms play critical roles in cell survival during inflammatory conditions, can be activated simultaneously (47), and have been explored as targeted therapeutic strategies across various cancer types (48). The fact that 3-MA, an autophagy inhibitor, did not suppress mTOR expression further supports the notion that mTOR activation in this context is not merely a feedback response to autophagy inhibition but may be driven by alternative mechanisms, such as amino acid sensing or ERK/MAPK signaling. An alternative interpretation highlights that the restricted observational timeframe (6 hr post-LPS) limits insight into NRG's long-term therapeutic effects and fails to capture the evolving interplay between autophagy and PI3K/Akt/mTOR signaling as sepsis advances. This short-term focus leaves unresolved whether NRG's early induction of autophagy (13) is counteracted by mTOR-mediated suppression in later stages, underscoring the need for extended temporal studies to map these dynamic interactions. While NRG enhances protective autophagy (via Beclin-1 and LC3 up-regulation) in early sepsis according to our immunohistochemistry data, the observed transcriptional activation of PI3K/Akt/mTOR raises unanswered questions about its functional impact

on autophagy inhibition in later stages. To address this, future studies should integrate longitudinal assessments (e.g., after 9 hr) with protein-level validation (e.g., Western blot for phosphorylated mTOR, Akt, and PI3K) to map the temporal interplay between pathway activation and autophagy dynamics. Such investigations could clarify the therapeutic window for NRG and inform strategies to synergize autophagy induction with mTOR modulation to optimize renal protection in the dynamic pathophysiology of sepsis. In addition, while NRG treatment increased the expression of PI3K, Akt, and mTOR transcripts, as well as autophagy-associated markers, mRNA levels do not necessarily reflect pathway activation or protein activity. Since signaling activity within the PI3K/Akt/mTOR cascade is primarily regulated through post-translational modifications, particularly protein phosphorylation, the functional status of this pathway could not be conclusively determined in the current study. Therefore, the observed changes in gene expression should be considered supportive but not definitive evidence of pathway involvement in the renoprotective effects of NRG. We suggest that our findings should be interpreted as evidence of altered gene expression rather than definitive activation of the PI3K/Akt/mTOR signaling cascade. Furthermore, the apparent coexistence of increased autophagy-related markers and elevated PI3K/Akt/mTOR gene expression may reflect a dynamic, time-dependent adaptive response during the early phase of sepsis-induced kidney injury. Overall, our findings highlight a more complex interplay between mTOR and autophagy in SI-AKI, in which NRG appears to restore metabolic activity and cellular homeostasis by coordinating both pathways.

NRG is known for its broad pharmacological activities—particularly its antioxidant and anti-inflammatory effects—which play a key role in its protective action against acute kidney injury (42). Our study demonstrates that NRG provides strong antioxidant, anti-inflammatory, and kidney-protective effects in SI-AKI. Exposure to LPS increased oxidative stress, as evidenced by higher MDA levels and reduced catalase activity, and elicited a significant inflammatory response, as indicated by elevated TNF-α levels. These pathological alterations were accompanied by elevated levels of NGAL and KIM-1, well-established biomarkers of renal injury, which are consistently elevated in SI-AKI (49). The rise in these markers underscores the severity of kidney damage, reflecting impaired tubular function and structural integrity in response to systemic inflammation and oxidative stress. Treatment with NRG effectively counteracted these harmful effects, reducing MDA and TNF-α levels while restoring catalase activity, which correlated with improved NGAL and KIM-1 levels. Interestingly, when autophagy was inhibited with 3-MA, NRG's protective effects remained unchanged, suggesting that its ability to reduce oxidative stress and inflammation is linked to the regulation of autophagy in the early stages of sepsis. These findings highlight NRG's potential as a promising therapeutic agent for protecting kidney function in sepsis-induced injury.

Moreover, further analysis of kidney function demonstrates that an increase in BUN and creatinine in the LPS group confirms severe renal impairment, likely due to inflammation, oxidative stress, and metabolic dysregulation. However, NRG treatment restores kidney function, reducing both BUN and creatinine levels, suggesting its protective effect against LPS-induced nephrotoxicity. Interestingly, the inhibition of autophagy with 3-MA does not reverse these beneficial effects, indicating that NRG's renoprotective properties may function independently of autophagy regulation. Additionally, the observed reduction in serum uric acid levels in the LPS group was followed by restoration in the LPS+NRG group. Taken together, these findings support the potential of NRG as a therapeutic agent to prevent kidney dysfunction in sepsis, possibly through mechanisms involving antioxidant, anti-inflammatory, and metabolic regulatory pathways.

Conclusion

This study demonstrates that NRG provides significant protection against SI-AKI by enhancing autophagy markers (Beclin-1, LC3) and activating the PI3K/Akt/mTOR pathway early in the course of SI-AKI, thereby attenuating oxidative stress, inflammation, and renal dysfunction.

Our findings reveal that NRG restores cellular homeostasis in SI-AKI, preserving tissue architecture and reducing injury biomarkers, such as KIM-1 and NGAL. However, this study has several limitations, including a short-term observation window (6 hr post-LPS), which does not capture the long-term consequences of NRG treatment. Therefore, further investigation into NRG-enhanced autophagy in the later stages of sepsis and the effects of increased protein levels in the PI3K/Akt/mTOR pathway is warranted. Moreover, although NRG's dual modulation of autophagy and PI3K/Akt/mTOR signaling was observed within the first 6 hr of sepsis, the precise molecular crosstalk between these pathways remains unclear. Together, these findings position NRG as a promising therapeutic candidate for SI-AKI and warrant further exploration to unlock its full potential in critical care settings.

Acknowledgment

The authors disclosed receipt of the following financial support for the research, authorship, and/or publication of this article: This study has been supported by a grant from the Research and Technology Department of Erciyes University (grant number FBA-2021-11235). Moreover, we would like to extend our sincere gratitude to the Erciyes University Drug Application and Research Center for their invaluable support in conducting some of our experiments. Their expertise and resources significantly contributed to the success of this study. We also appreciate the collaborative spirit and technical assistance provided by the center's team.

Ethics Approval

The experimental protocol performed in the present study was approved by Erciyes University's Experimental Animal and Local Ethics Committee (number 21/102/2021).

Availability of Data and Material

The datasets generated and/or analyzed in the current study are not publicly available due to privacy concerns but are available from the corresponding author upon reasonable request.

Authors' Contributions

The authors declare that all data were generated in-house and that no paper mill was used. AT A, Z Y, and E K designed the study; A T helped secure funding, and AT A, Z

Y, and E K administered the drug. AT A, E K, N D, and E O contributed to data analysis. AT A, Ş V, and E K performed histological and immunohistochemical analyses; N D, E O, M S, and D K conducted ELISA assays. AT A wrote the manuscript. AT A, D K, and Z D revised the final version of the manuscript.

Conflicts of Interest

The authors declare no conflicts of interest in the publication of this article.

Declaration

We acknowledge the use of ChatGPT (OpenAI) solely for English language editing, including grammar, spelling, and clarity improvements. No content, data, interpretations, or scientific conclusions were generated by the AI tool.

References

1. Deng Z, He M, Hu H, Zhang W, Zhang Y, Ge Y, *et al.* Melatonin attenuates sepsis-induced acute kidney injury by promoting mitophagy through SIRT3-mediated TFAM deacetylation. Autophagy 2024; 20: 151-165.
2. Bellomo R, Kellum JA, Ronco C, Wald R, Martensson J, Maiden M, *et al.* Acute kidney injury in sepsis. Intensive Care Med 2017; 43: 816-828.
3. Peerapornratana S, Manrique-Caballero CL, Gomez H, Kellum JA. Acute kidney injury from sepsis: Current concepts, epidemiology, pathophysiology, prevention and treatment. Kidney Int 2019; 96: 1083-1099.
4. Gao L, Zhong X, Jin J, Li J, Meng X-m. Potential targeted therapy and diagnosis based on novel insight into growth factors, receptors, and downstream effectors in acute kidney injury and acute kidney injury-chronic kidney disease progression. Signal Transduct Target Ther 2020; 5: 9.
5. Kuwabara S, Goggins E, Okusa MD. The Pathophysiology of sepsis-associated AKI. Clin J Am Soc Nephrol 2022; 17: 1050-1069.
6. Romero Pajaro BJ, Caicedo Sánchez DC, Vélez Lora M, Mena Gasca JF, Ochoa Guette DA, Romero Martínez G, *et al.* Biomarker-based diagnosis and risk stratification in sepsis-associated acute kidney injury: From molecular mechanisms to multimarker panels. Diagnostics (Basel) 2026; 16: 1262.
7. Filomeni G, De Zio D, Cecconi F. Oxidative stress and autophagy: The clash between damage and metabolic needs. Cell Death Differ 2015; 22: 377-388.
8. Wu H, Cui J, Huang J, Feng Y, Zhao J, Zhu Y, *et al.* Cell death signaling and immune regulation: New perspectives on targeted therapy for sepsis. Cell Mol Biol Lett 2025; 30: 99.
9. Kimura T, Isaka Y, Yoshimori T. Autophagy and kidney inflammation. Autophagy 2017; 13: 997-1003.
10. Huang G, Bao J, Shao X, Zhou W, Wu B, Ni Z, *et al.* Inhibiting pannexin-1 alleviates sepsis-induced acute kidney injury via decreasing NLRP3 inflammasome activation and cell apoptosis. Life Sci 2020; 254: 117791.
11. Wu Z, Deng J, Zhou H, Tan W, Lin L, Yang J. Programmed cell death in sepsis associated acute kidney injury. Front Med (Lausanne) 2022; 9: 883028.
12. Mei S, Livingston M, Hao J, Li L, Mei C, Dong Z. Autophagy is activated to protect against endotoxic acute kidney injury. Sci Rep 2016; 6: 22171.
13. Hsiao H-W, Tsai K-L, Wang L-F, Chen Y-H, Chiang P-C, Chuang S-M, *et al.* The decline of autophagy contributes to proximal tubular dysfunction during sepsis. Shock 2012; 37: 289-296.
14. Hu S, Zhang Y, Zhang M, Guo Y, Yang P, Zhang S, *et al.* Aloperine protects mice against ischemia-reperfusion (IR)-induced renal injury by regulating PI3K/AKT/mTOR signaling and AP-1 activity. Mol Med 2016; 21: 912-923.
15. Liu X, Ai F, Li H, Xu Q, Mei L, Miao J, *et al.* Anti-inflammatory effects of shenfu injection against acute lung injury through inhibiting HMGB1-NF-κB pathway in a rat model of endotoxin shock. Evid Based Complement Alternat Med 2019; 2019: 9857683.
16. Saxton RA, Sabatini DM. mTOR signaling in growth, metabolism, and disease. Cell 2017; 169: 361-371.
17. Sarkar S. Regulation of autophagy by mTOR-dependent and mTOR-independent pathways: Autophagy dysfunction in neurodegenerative diseases and therapeutic application of autophagy enhancers. Biochem Soc Trans 2013; 41: 1103-1130.
18. Ren D, Liu Q, Liao H, Wang M, Wang Y, Guo W, *et al.* Inflammation, cell death, and lncRNAs: Unraveling the mechanisms of sepsis-associated acute kidney injury. Front Immunol 2026; 17: 1710624.
19. Wang Y, Zong L, Zhu M, Li J, Xu J, Li H, *et al.* Current status and future prospects of research on sepsis-related acute kidney injury. Int J Mol Sci 2026; 27: 1315.
20. Xu J, Lu C, Liu Z, Zhang P, Guo H, Wang T. Schizandrin B protects LPS-induced sepsis via TLR4/NF-κB/MyD88 signaling pathway. Am J Transl Res 2018; 10: 1155-1163.
21. Susantitaphong P, Siribamrungwong M, Doi K, Noiri E, Terrin N, Jaber BL. Performance of urinary liver-type fatty acid-binding protein in acute kidney injury: A meta-analysis. Am J Kidney Dis 2013; 61: 430-439.
22. Zdziechowska M, Glubas-Gozdowska A, Poliwczak AR, Franczyk B, Kidawa M, Zielinska M, *et al.* Serum NGAL, KIM-1, IL-18, L-FABP: New biomarkers in the diagnostics of acute kidney injury (AKI) following invasive cardiology procedures. Int Urol Nephrol 2020; 52: 2135-2147.
23. Pan HC, Yang SY, Chiou TT, Shiao CC, Wu CH, Huang CT, *et al.* Comparative accuracy of biomarkers for the prediction of hospital-acquired acute kidney injury: A systematic review and meta-analysis. Crit Care 2022; 26: 349.
24. Shaaban MF, Mohamed WA. Determinants of hepcidin levels in sepsis-associated acute kidney injury: Impact on pAKT/PTEN pathways? J Immunotoxicol 2016; 13: 751-757.
25. Chen R, Qi QL, Wang MT, Li QY. Therapeutic potential of naringin: An overview. Pharm Biol 2016; 54: 3203-3210.
26. Caglayan C, Temel Y, Kandemir FM, Yildirim S, Kucukler S. Naringin protects against cyclophosphamide-induced hepatotoxicity and nephrotoxicity through modulation of oxidative stress, inflammation, apoptosis, autophagy, and DNA damage. Environ Sci Pollut Res Int 2018; 25: 20968-20984.
27. Elsawy H, Alzahrani AM, Alfwuaires M, Abdel-Moneim AM, Khalil M. Nephroprotective effect of naringin in methotrexate induced renal toxicity in male rats. Biomed Pharmacother 2021; 143: 112180.
28. Yilmaz E, Acar G, Onal U, Erdogan E, Baltaci AK, Mogulkoc R. Effect of 2-week naringin supplementation on neurogenesis and BDNF levels in ischemia-reperfusion model of rats. Neuromolecular Med 2024; 26: 4.
29. Tsai YC, Cheng PY, Kung CW, Peng YJ, Ke TH, Wang JJ, *et al.* Beneficial effects of magnolol in a rodent model of endotoxin shock. Eur J Pharmacol 2010; 641: 67-73.
30. Zhao Y, Feng X, Li B, Sha J, Wang C, Yang T, *et al.* Dexmedetomidine protects against lipopolysaccharide-induced acute kidney injury by enhancing autophagy through inhibition of the PI3K/AKT/mTOR pathway. Front Pharmacol 2020; 11: 128.
31. Ceylan T, Kaymak E, Akin AT, Yakan B. The ameliorative effects of caffeic acid phenethyl Ester in cisplatin-induced nephrotoxicity: Assessment of the oxidative stress an inflammation. Int J Morphol 2021; 39: 612-618.
32. Akin AT, Ünsal M, Ceylan T, Kaymak E, Öztürk E, Kuloğlu N, *et al.* Protective effect of melatonin on cisplatin induced acute kidney injury: Role of regulation of heat shock proteins expressions. Indian J Exp Biol 2023; 61: 687-696.
33. Ozturk E, Karabulut D, Akin AT, Kaymak E, Kuloglu N, Yakan B. Evaluation by different mechanisms of the protective effects of vitamin B12 on methotrexate nephrotoxicity. J Mol Histol 2022; 53: 133-143.
34. Akin AT, Öztürk E, Kaymak E, Karabulut D, Yakan B. Therapeutic effects of thymoquinone in doxorubicin-induced

hepatotoxicity via oxidative stress, inflammation and apoptosis. Anat Histol Embryol 2021; 50: 908-917.
35. Ayhan H, Adiguzel C, Bayram KK, Akin AT, Apaydin FG, Kalender Y. Effect of propolis supplementation on cadmium toxicity associated with renal and hepatic dysfunction in rats. J Trace Elem Med Biol 2025; 87: 127587.
36. Ceylan T, Akin AT, Karabulut D, Tan FC, Taşkiran M, Yakan B. Therapeutic effect of thymoquinone on brain damage caused by nonylphenol exposure in rats. J Biochem Mol Toxicol 2023; 37: e23471.
37. Peerapornratana S, Manrique-Caballero CL, Gómez H, Kellum JA. Acute kidney injury from sepsis: Current concepts, epidemiology, pathophysiology, prevention and treatment. Kidney Int 2019; 96: 1083-1099.
38. Jin YH, Li ZT, Chen H, Jiang XQ, Zhang YY, Wu F. Effect of dexmedetomidine on kidney injury in sepsis rats through TLR4/MyD88/NF-κB/iNOS signaling pathway. Eur Rev Med Pharmacol Sci 2019; 23: 5020-2025.
39. Keir I, Kellum JA. Acute kidney injury in severe sepsis: Pathophysiology, diagnosis, and treatment recommendations. J Vet Emerg Crit Care (San Antonio) 2015; 25: 200-209.
40. Bellomo R, Kellum JA, Ronco C, Wald R, Martensson J, Maiden M, *et al*. Acute kidney injury in sepsis. Intensive Care Med 2017; 43: 816-828.
41. McCann MR, Fry C, Maile MD, Farkash EA, Cummings BC, Flott TL, *et al*. Early sepsis metabolic changes in kidney and liver precede clinical evidence of organ dysfunction. Am J Respir Cell Mol Biol 2025; 73: 299-309.
42. Amini N, Maleki M, Badavi M. Nephroprotective activity of naringin against chemical-induced toxicity and renal ischemia/reperfusion injury: A review. Avicenna J Phytomed 2022; 12: 357-370.
43. Chtourou Y, Aouey B, Aroui S, Kebieche M, Fetoui H. Anti-apoptotic and anti-inflammatory effects of naringin on cisplatin-induced renal injury in the rat. Chem Biol Interact 2016; 243: 1-9.
44. Liu N, Lei R, Tang MM, Cheng W, Luo M, Xu Q, *et al*. Autophagy is activated to protect renal tubular epithelial cells against iodinated contrast media-induced cytotoxicity. Mol Med Rep 2017; 16: 8277-8282.
45. Cui N, Chen Z, Yu Z, Lv X, Hu Z. PTX3 mediates PI3K/AKT/mTOR signaling to downregulate apoptosis and autophagy to attenuate myocardial injury in sepsis. PeerJ 2024; 12: e17263.
46. He L, Zhang J, Zhao J, Ma N, Kim SW, Qiao S, *et al*. Autophagy: The last defense against cellular nutritional stress. Adv Nutr 2018; 9: 493-504.
47. Roy T, Banang-Mbeumi S, Boateng ST, Ruiz EM, Chamcheu RN, Kang L, *et al*. Dual targeting of mTOR/IL-17A and autophagy by fisetin alleviates psoriasis-like skin inflammation. Front Immunol 2022; 13: 1075804.
48. Huang HY, Li KN, Lau HC, Hsuen CY, Cong N, Zhang M. Dual inhibition of autophagy and PI3K/mTOR pathway as a potential therapeutic strategy against laryngeal squamous cell carcinoma. Transl Cancer Res 2022; 11: 1078-1088.
49. Pei Y, Zhou G, Wang P, Shi F, Ma X, Zhu J. Serum cystatin C, kidney injury molecule-1, neutrophil gelatinase-associated lipocalin, klotho and fibroblast growth factor-23 in the early prediction of acute kidney injury associated with sepsis in a Chinese emergency cohort study. Eur J Med Res 2022; 27: 39.